Electronic Supplementary Material for "Imitation dynamics of vaccination behaviour on social networks"

Feng Fu, Daniel I. Rosenbloom, Long Wang, Martin A. Nowak

June 30, 2010

Contents

1 Epidemic modeling

We use the Susceptible-Infected-Recovered (SIR) model for the disease transmission process. The SIR model is appropriate for a large class of infectious diseases such as influenza and measles, and is widely studied in epidemiology (Keeling & Eames, 2005). In this model, the population is divided to three classes: susceptible individuals (S), who are healthy but can catch the disease if exposed to infected individuals; infected individuals (I), who have the disease and can pass it on; and recovered individuals (R), who acquire immunity to the disease.

1.1 SIR model in well-mixed populations

Suppose the disease transmission rate (per person) is r, and the rate of recovery from infection is g. The fraction of susceptible, infected, and recovered individuals is S, I, and R, respectively, in a population of size N. For well-mixed populations, the time evolution of the population states can be expressed as the following deterministic ordinary differential equations:

$$\frac{dS}{dt} = -rNSI, \tag{1}$$

$$\frac{dI}{dt} = rNSI - gI, \tag{2}$$

$$\frac{dR}{dt} = gI. \tag{3}$$

The initial condition for an epidemic introduced by one infected individual is $S(0) = 1 - 1/N \approx 1$, $I(0) = 1/N$, and $R(0) = 0$. Denote rN/g by R_0, commonly called the "basic reproduction ratio" (Heffernan et al., 2005). Here R_0 is the mean number of secondary infections caused by a single infected individual, during his/her entire infectious period, in a completely susceptible population.

Dividing Eq. (1) by Eq. (3), we obtain

$$\frac{dS}{dR} = -R_0 S. \tag{4}$$

Integrating above equation from time 0 to ∞, we get the transcendental equation for the final epidemic size $R(\infty)$:

$$S(\infty) = S(0)e^{-R_0[R(\infty)-R(0)]}. \tag{5}$$

Using the initial condition $S(0) \approx 1$ and $R(0) = 0$, and the final state $I(\infty) = 0$ and $S(\infty) = 1 - R(\infty)$, we obtain:

$$R(\infty) = 1 - e^{-R_0 R(\infty)}. \tag{6}$$

$R(\infty)$ is the final fraction of individuals who had been infected during the epidemic outbreak, *i.e.*, the final epidemic size, which can be calculated numerically from the above equation. Differentiating both sides of Eq. (6) with respect to $R(\infty)$, we can see that the final size is positive if and only if $R_0 > 1$. If $R_0 < 1$, the disease does not spread.

If we consider preemptive vaccination by supposing that a proportion x of the population initially vaccinated, Eq. (6) can be rewritten as

$$R(\infty) = (1 - x)(1 - e^{-R_0 R(\infty)}). \tag{7}$$

Increasing vaccination decreases the final size of the epidemic, and if $x > x_h = 1 - \frac{1}{R_0}$, we have $R(\infty) = 0$. The critical value x_h is called the "herd immunity threshold," above which the infection does not spread through the population. For vaccine-preventable diseases, herd immunity therefore grants indirect protection to unvaccinated individuals; it is a public good that vaccinated individuals create and unvaccinated individuals can free-ride on.

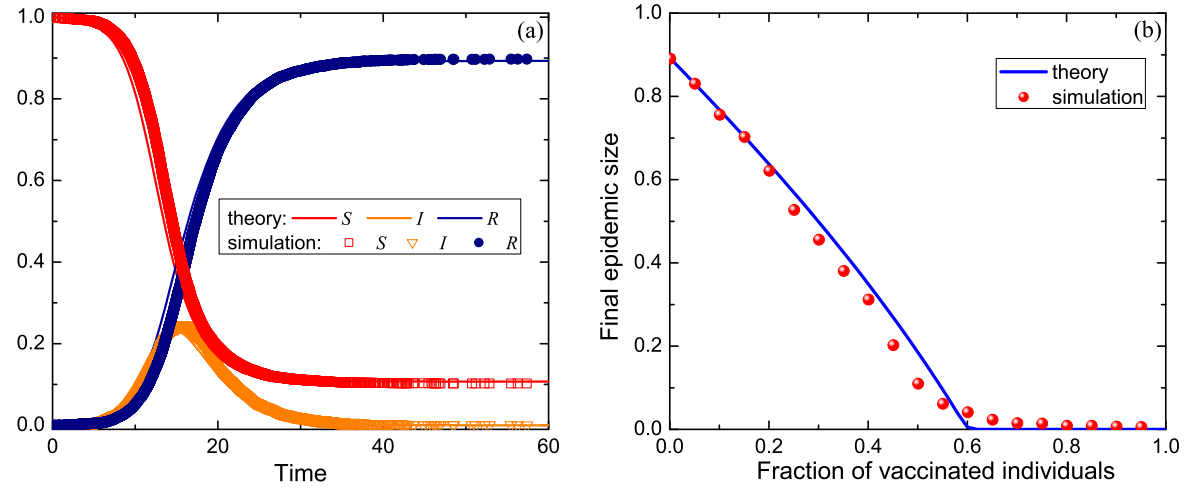

Figure S1: Epidemic spreading in well-mixed populations. (a) The fractions of susceptible, infected, and recovered individuals as a function of time. (b) The fraction of individuals who had been infected as a function of preemptive vaccination level. The solid line in panel (b) is numerically determined from Eq. (7). Parameters: (a) $N = 10^4$, $g = 1/3$ day^{-1}, $R_0 = 2.5$, the number of initial infection seeds $I_0 = 10$; (b) $N = 1000$, $R_0 = 2.5$, $I_0 = 5$, results averaged over 50 runs.

We use the Gillespie algorithm in our stochastic simulations (detailed in section 1.3). To lower the chance that an epidemic outbreak fails merely due to stochastic effects, we make the initial number of infection seeds I_0 more than one. Figure S1 shows the epidemic spreading in well-mixed populations. For $R_0 = 2.5$, the final epidemic size with zero vaccination is ~ 0.893, and the herd immunity threshold is $x_h = 0.6$. Our simulation results agree with the deterministic model given by Eqs.(1)–(3) (figures S1a and S1b). Note that for intermediate initial fractions of vaccinated individuals ($0.2 < x < 0.6$), the final epidemic size resulting from simulations is lower that than the analytical prediction (Eq. 7). Stochastic effects due to finite infection size cause this deviation.

1.2 Epidemic spreading in structured populations

It is not typically possible to derive explicit equations for epidemic spreading in structured populations (Keeling & Eames, 2005), so we use stochastic simulations. It is widely accepted that population structure can substantially alter epidemiological dynamics from the well-mixed case (Newman, 2003). To identify only the effects of population structure, we must calibrate epidemic parameters to ensure that infection risk is equal in all structures examined (Perisic & Bauch, 2008). We use as the base case a well-mixed population with $R_0 = 2.5$, which is within the typical R_0 values for influenza ($1.5 < R_0 < 3$). We fix the recovery rate at $g = 1/3$ day^{-1} (so the mean infectious period is 3 days), and choose the transmission rate r such that the final epidemic size is that of the well-mixed population without vaccination.

We simulated populations structured as square lattices, Erdős-Rényi random graphs (Erdős & Rényi, 1959), and Barabási-Albert scale-free networks (Barabási & Albert, 1999). To account for the increased risk that individuals with many connections face, we assume that the infection probability of a susceptible individual i is proportional to the number of her infected neighbors $N_I(i)$. The transition rate from S to I for individual i is then $rN_I(i)$ (Keeling & Eames, 2005).

For lattice populations, the final epidemic size shows a clear phase transition from zero to one with increasing r values (figure S2a). For low r values, the epidemic spreading is inhibited due to local spatial clustering effects. We select $r = 0.46$ day^{-1}person^{-1}, which gives a final epidemic size of ~ 0.893, approximately equal to the base case. Using this transmission rate, we simulate the effect of preemptive, random vaccination on the epidemic (figure S2b). The final epidemic size decreases more precipitously than in the well-mixed case (cf. figures S1b and S2b). At vaccination levels greater than about 0.6, the disease cannot

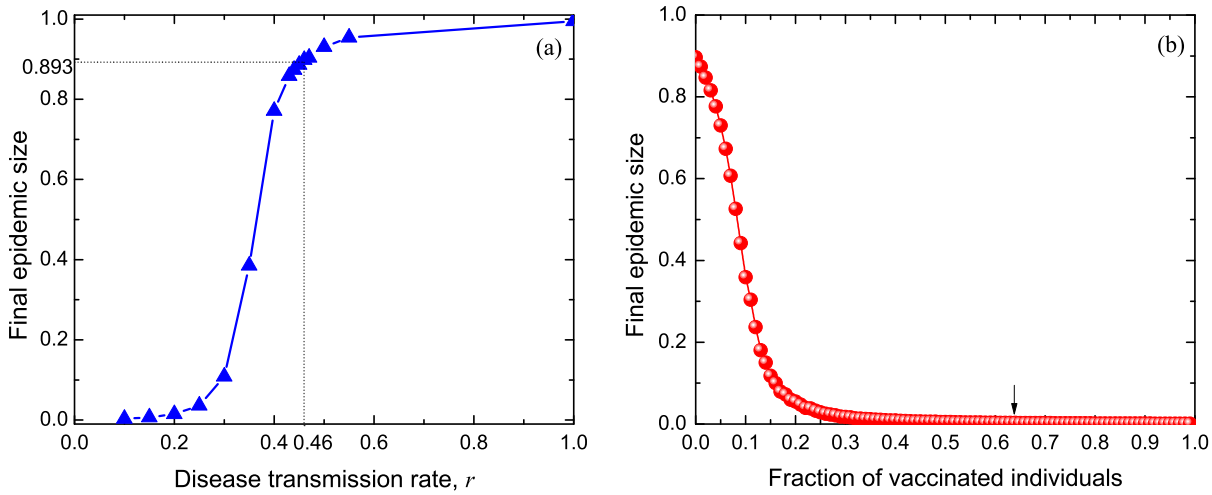

Figure S2: Epidemic spreading in lattice populations. (a) The final epidemic size is shown as a function of the transmission rate r with zero vaccination coverage. (b) The final epidemic size as a function of vaccination level (preemptive, random vaccination). The arrow notes where vaccination brings the final epidemic size below 0.2% (twice the size of initial inoculum), representing an approximate herd immunity threshold. Parameters: $N = 100 \times 100$ with von Neumann neighborhood (four adjacent neighbors), (a)-(b) $g = 1/3$ day^{-1}, $I_0 = 10$, (b) $r = 0.46$ day^{-1}person^{-1}. Results are averaged over 100 runs.

persist in the population (marked by the arrow in figure S2b).

Compared to spatial lattices, both the absence of local clustering and the presence of degree heterogeneity (different individuals can have different numbers of neighbors) in random graphs and scale-free networks make it easier for the disease to spread at lower transmission rates and higher vaccination rates (figures S3 and S4). Using the same method as above, we choose $r = 0.51$ day^{-1}person^{-1} for random graphs (figure S3a) and $r = 0.55$ day^{-1}person^{-1} for scale-free networks (figure S4a). Notice that even for vanishingly small r values, scale-free networks are fragile to epidemic attacks, consistent with previous findings (Pastor-Satorras & Vespignani, 2001). Accordingly, the vaccination level needed to contain the disease is the highest among all the population structures we studied (figure S4).

1.3 Stochastic simulation procedure: Gillespie algorithm

We use the Gillespie algorithm to simulate the epidemiological process (Gillespie, 1977). The simulation procedure works as follows:

Step 1: At time t, calculate each susceptible and infected individual's transition rate, $p_i(t)$. The rate at which a susceptible individual becomes infected is $p_i(t) = r \times$ number of infected neighbors. The rate at which an infected individual recovers from the disease is $p_i(t) = g$. The total transition rate is $\lambda(t) = \sum_i p_i(t)$.

Step 2: The time at which the next transition event occurs is $t' = t + \Delta t$, where Δt is sampled from an exponential distribution with mean $\frac{1}{\lambda(t)}$. (Generate a uniform random number $u \in [0, 1)$. Then the time interval is $\Delta t = -\frac{\ln(1-u)}{\lambda(t)}$.)

Step 3: Choose the individual whose state changes at time t' by sampling proportional to $p_i(t)$. Generate a uniform random number $v \in [0, 1)$. If $\sum_{j=1}^{k-1} p_j(t)/\lambda(t) < v < \sum_{j=1}^{k} p_j(t)/\lambda(t)$, then individual k is chosen to change state. (Define $\sum_{j=1}^{0} p_j(t)/\lambda(t) = 0$.)

Step 4: Repeat Steps 1–3 until the number of infected individuals $I(t)$ is zero, or stop after a predetermined time period.

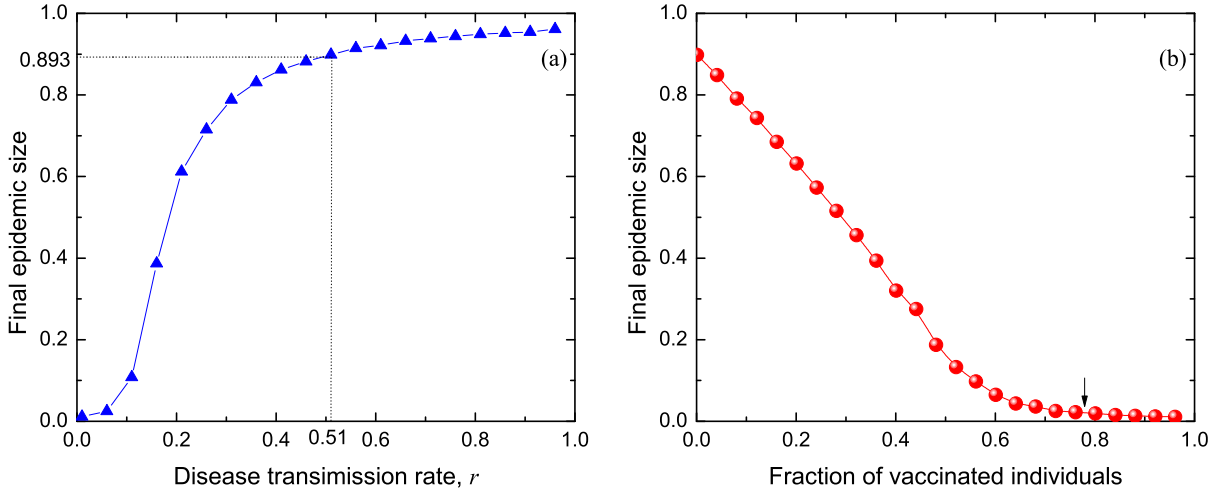

Figure S3: Epidemic spreading in Erdős-Rényi random networks. (a) The final epidemic size as a function of the disease transmission rate r with zero vaccination coverage. (b) The final epidemic size as a function of the vaccination level (preemptive, random vaccination). The arrow notes where vaccination brings the final epidemic size below 2%, representing an approximate herd immunity threshold. Parameters: (a)-(b) $N = 1000$, average degree $\bar{k} = 4$, $I_0 = 10$, $g = 1/3$ day^{-1}; (b) $r = 0.51$ day^{-1}person^{-1}. Results are averaged over 100 runs.

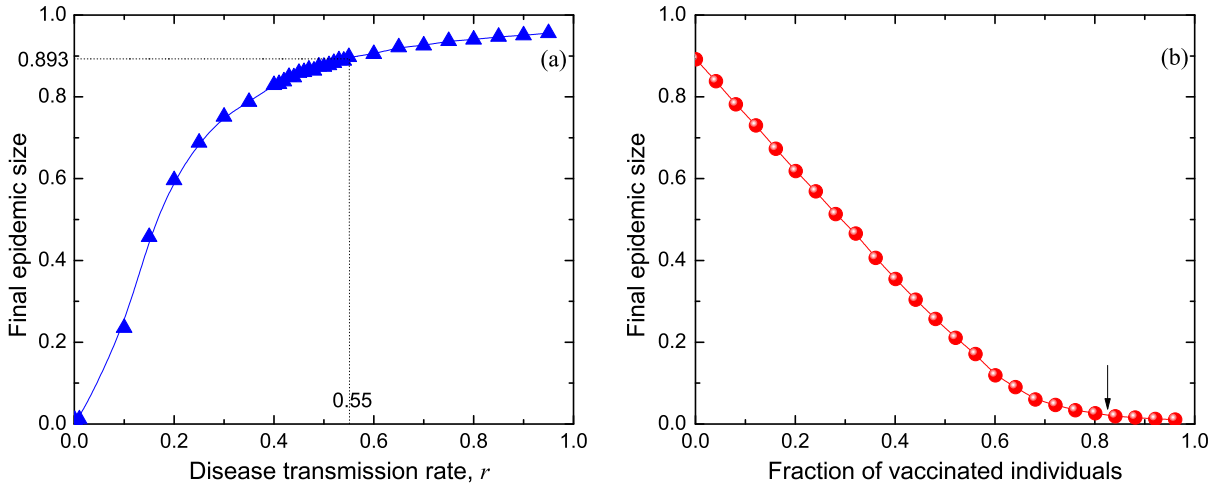

Figure S4: Epidemic spreading in Barabási-Albert scale-free networks. (a) The final epidemic size as a function of the disease transmission rate r with zero vaccination coverage. (b) The final epidemic size as a function of the vaccination level (preemptive, random vaccination). The arrow notes where vaccination brings the final epidemic size below 2%, representing an approximate herd immunity threshold. Parameters: (a)-(b) $N = 1000$, average degree $\bar{k} = 4$, $I_0 = 10$, $g = 1/3$ day^{-1}; (b) $r = 0.55$ day^{-1}person^{-1}. Results are averaged over 100 runs.

2 Costs of vaccination and infection in typical influenza season

Values of c are supported by data from Galvani et al. (2007), which estimates the cost of health outcomes: Vaccination costs $37 on average, and the expected cost of infection for non-vaccinated individuals is given for four cases:

- Young individuals (< 65 years) during normal seasons: $570
- Elderly individuals (≥ 65 years) during normal seasons: $4,160
- Young individuals during pandemics (*e.g.,* 1918 influenza): $21,220
- Elderly individuals during pandemics: $16,170

To represent the imperfect effectiveness of vaccination (roughly 80% effectiveness for the young and 60% for the elderly), we scaled the vaccination cost by $\frac{1}{80\%} = 1.25$ and $\frac{1}{60\%} = 1.67$ for each group, respectively. The relative vaccination costs (as a fraction of infection costs) are then:

- Young, normal seasons: $c = 0.08$
- Elderly, normal seasons: $c = 0.01$
- Young, pandemics: $c = 0.002$
- Elderly, pandemics: $c = 0.004$

Based on these estimates, we propose that it is reasonable to use values of c in the range 0.001 to 0.1 in our model to discuss influenza.

3 Nash equilibrium and social optimum

3.1 Nash equilibrium

Here we demonstrate the existence and uniqueness of the Nash equilibrium (*i.e.*, individual rational optimum) in the vaccination game, provided that individuals have perfect knowledge of the vaccination coverage level and infection risk. Propose strategy x (representing the probability of vaccination) to be a Nash equilibrium: if most of the population plays strategy x, then individuals adopting a different strategy y can do no better than the resident. For an ϵ-size invasion ($\epsilon \ll 1$), the new vaccination coverage is $p := x(1-\epsilon)+y\epsilon$. The expected payoff to strategy y is then

$$E(y, p) = -yc + (1 - y)\{[1 - w(p)] \cdot 0 + w(p) \cdot (-1)\}, \tag{8}$$

where $w(p)$ is the infection risk for an unvaccinated individual, given that a proportion p of the population is vaccinated. Strategy x is Nash if it is a best response to itself, which requires the conditions

$$\left.\frac{\partial E(y, p)}{\partial y}\right|_{y=x} = w(x) - c - \epsilon(1 - x)w'(x) = 0, \tag{9}$$

$$\left.\frac{\partial^2 E(y, p)}{\partial y^2}\right|_{y=x} = 2\epsilon w'(x) - (1 - x)\epsilon^2 w''(x) \leq 0. \tag{10}$$

Note that $w(x)$ strictly decreases with x, until x reaches the herd immunity threshold x_h. For $x < x_h$, the inequality (10) is therefore strict for a sufficiently small invasion ϵ, and so higher-order conditions are not required. Also, for small invasions, the ϵ term in Eq. (9) can be safely neglected. The vaccination cost falls into one of three ranges:

- *Case 1,* $0 < c \leq w(0)$. Since $w(x)$ strictly decreases, there is a unique x^* that solves $w(x^*) = c$. This value x^* is the Nash equilibrium.

- *Case 2,* $c > w(0)$. As the derivative in Eq. (9) is negative, the best response is x as small as possible; that is, the pure Nash equilibrium $x^* = 0$.

- *Case 3,* $c \leq 0$. As the derivative in Eq. (9) is positive, the best response is x as large as possible; that is, the pure Nash equilibrium $x^* = 1$.

Moreover, strictness of the inequality (10) in Case 1 implies that an alternative strategy $y \neq x^*$ does strictly worse, meaning that the Nash equilibrium is also evolutionarily stable (Hofbauer and Sigmund, 1998).

Furthermore, we can show that the unique Nash equilibrium x^* in this game is globally stable. For any proportion $\epsilon \in (0, 1)$ of individuals playing strategy $y \neq x^*$, we always have

$$\Delta E = E(x^*, p) - E(y, p) = (x^* - y)\left[w(p) - c\right] > 0, \tag{11}$$

which means that the strategy x^* is favored against any alternative strategy at any frequency.

3.1.1 Calculating the Nash equilibrium from epidemiological parameters

For well-mixed populations, $w(x)$ is the ratio of the number of individuals who acquired disease, $R(\infty)$, to the total number of susceptible individuals, $S(0)$. Therefore we obtain

$$w(x) = \frac{R(\infty)}{1 - x} = 1 - e^{-R_0 R(\infty)}. \tag{12}$$

Using Eq. (7) and the Nash condition $w(x^*) = c$, we have $e^{-R_0 R(\infty)} = 1 - c$ and $R(\infty) = (1 - x^*)c$. We then obtain the Nash Equilibrium

$$x^* = 1 + \frac{\ln(1 - c)}{cR_0}, \tag{13}$$

which is plotted in figure S5. This equation holds for $0 < c \leq w(0)$ (recall, $w(0) = 1 - e^{-R_0 w(0)}$). Cases 2 and 3 above cover the alternatives.

3.2 Social optimum

The population's optimal vaccination coverage can be obtained by minimizing the total expected cost from both vaccination and infection. If a fraction x of the population is vaccinated, the expected cost is

$$\begin{aligned} E(x) &= N\left\{xc + (1 - x)\left\{0 \cdot [1 - w(x)] + w(x) \cdot 1\right\}\right\}, & (14)\\ &= N\left[xc + R(\infty)\right], & (15)\\ &= N\left[xc + (1 - x)(1 - e^{-R_0 R(\infty)})\right]. \end{aligned}$$

We show that the social optimum is exactly the herd immunity threshold, $x_h = 1 - 1/R_0$.

For x above x_h, the final epidemic size $R(\infty)$ is zero. $E(x)$ therefore increases as x rises above x_h.

For x below x_h, $\frac{dE(x)}{dx} = N\left[c + \frac{dR(\infty)}{dx}\right]$. It is easy to show that $\frac{dR(\infty)}{dx} < 0$; that is, that final infection size decreases with vaccination coverage. Furthermore, differentiating both sides of Eq. (7) with respect to x, we obtain:

$$\frac{dR(\infty)}{dx} = -\frac{e^{R_0 R(\infty)} - 1}{e^{R_0 R(\infty)} - (1 - x)R_0}, \tag{16}$$

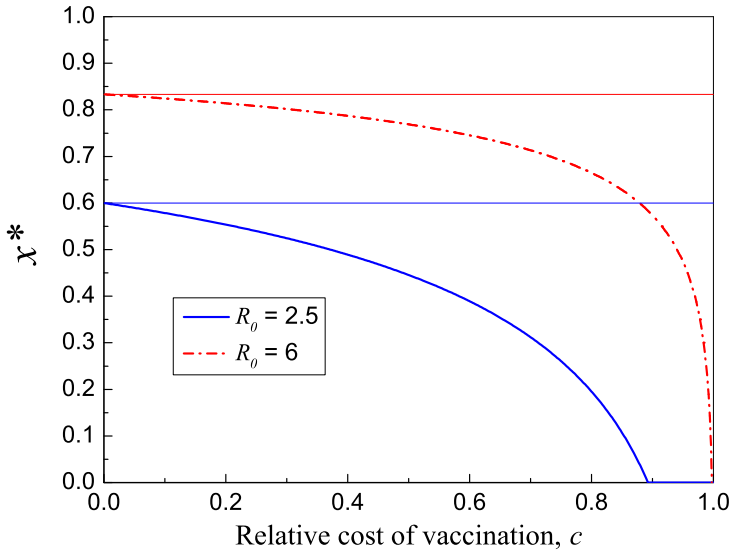

Figure S5: Nash equilibrium as a function of relative cost of vaccination cost c with different disease transmissibility R_0. The horizontal lines correspond to socially optimal vaccination levels.

which is guaranteed to be less than -1 for $(1-x)R_0 > 1$; *i.e.*, $x < x_h$. Hence we know that $\frac{dE(x)}{dx} = N\left[c + \frac{dR(\infty)}{dx}\right]$ is negative for $c < 1$ and $x < x_h$.

Since $E(x)$ decreases for $x < x_h$ and increases for $x > x_h$, the socially optimal vaccination level is precisely x_h.

For any $c \in (0, 1)$, the Nash equilibrium falls short of the social optimum, leading to the well-known dilemma of voluntary vaccination in a population of selfish, rational individuals.

3.3 Effects of R_0 on voluntary vaccination

For a fixed relative cost of vaccination, the Nash equilibrium increases with rising R_0 (figure S5): given a higher risk of infection, rational individuals are more likely to vaccinate. In the limiting case $R_0 \to \infty$, unvaccinated individuals cannot free-ride on the immunity generated by others, and so they eventually get infected. In this case, the Nash equilibrium and social optimum converge to 100% vaccination. For the opposite limiting case $R_0 \leq 1$, individuals have zero risk of infection, so that the Nash equilibrium and social optimum again agree — no one is vaccinated.

4 Evolution of vaccinating behavior in well-mixed populations

Above, we analyzed the vaccination dilemma from the perspective of classical game theory. Here we consider vaccination dynamics from an evolutionary game perspective. We derive a diffusion approximation for large populations of size N. Let m/N be the fraction of vaccinated individuals, who are immune from the seasonal infectious disease. Individuals imitate others based on the *pairwise comparison rule*, which preferentially copies others with higher payoffs (Traulsen et al., 2007). Each round, a randomly chosen individual i selects another random individual j as role model, and compares her own payoff to that of the role model. Individual i adopts the strategy of individual j with the probability given by the Fermi function

$$\phi(s_i \leftarrow s_j) = f(P_j - P_i) = \frac{1}{1 + \exp[-\beta(P_j - P_i)]}, \tag{17}$$

where β represents the intensity of selection. The population can change only if individuals i and j have different strategies. Hence, the probability that the number of vaccinated individuals increases from m to

	vaccinated	unvaccinated and infected	unvaccinated and healthy
fraction	x	$R(\infty)$	$1 - x - R(\infty)$
payoff	$P_A = -c$	$P_{B_1} = -1$	$P_{B_0} = 0$

Table 1: The fraction of individuals with different states and their corresponding payoffs.

$m+1$ (denoted T_m^+) and the probability that the number decreases from m to $m-1$ (denoted T_m^-) are

$$T_m^{\pm} = \frac{m}{N}\frac{N-m}{N}\left\{[1-w(m/N)]\frac{1}{1+e^{\mp\beta(P_A-P_{B_0})}} + w(m/N)\frac{1}{1+e^{\mp\beta(P_A-P_{B_1})}}\right\}, \tag{18}$$

where P_A is the payoff of vaccinated individuals, P_{B_0} the payoff of unvaccinated (and healthy) individuals, and P_{B_1} the payoff of unvaccinated (and infected) individuals (see Table 1).

For large populations (Traulsen et al., 2005), this process can be approximated by a stochastic differential equation with drift $T_m^+ - T_m^-$ and diffusion $\sqrt{(T_m^+ + T_m^-)/N}$, yielding

$$\dot{x} = x(1-x)\left\{[1-w(x)]\tanh\left[\frac{\beta}{2}(P_A - P_{B_0})\right] + w(x)\tanh\left[\frac{\beta}{2}(P_A - P_{B_1})\right]\right\} + \sqrt{\frac{x(1-x)}{N}}\xi \tag{19}$$

where $x = m/N$ is the fraction of vaccinated individuals and ξ is Gaussian white noise with variance one. For $N \to \infty$, the stochastic term vanishes. As a result, for large populations, we can use the deterministic approximation

$$\dot{x} = x(1-x)\left\{[1-w(x)]\tanh\left[\frac{\beta}{2}(-c-0)\right] + w(x)\tanh\left[\frac{\beta}{2}(-c+1)\right]\right\}. \tag{20}$$

At equilibrium where a fraction x is vaccinated, the fraction infected is expected to be $R(\infty)$ (as given in Eq. (7)), and the fraction that are successful free-riders (unvaccinated and healthy) is expected to be $1 - x - R(\infty)$ (see Table 1).

A. For small β, we have $\tanh(\beta x) \sim \beta x$. Thus Eq. (20) simplifies to

$$\begin{aligned}\dot{x} &= x(1-x)\left[-c[1-w(x)]\frac{\beta}{2} + w(x)\frac{\beta}{2}(1-c)\right] \\ &= \frac{\beta}{2}x(1-x)[w(x)-c].\end{aligned} \tag{21}$$

The replicator dynamics are recovered in this limit, $\beta \ll 1$, but with the time scale adjusted by a factor $\frac{\beta}{2}$. For any vaccination cost $0 < c < w(0)$, the system converges to the interior equilibrium $x^* = 1 + \ln(1-c)/(cR_0)$, which is evolutionarily stable as remarked above.

B. For large β:

B1. For $c \to 0$ ($c < 1/\beta$), $-\frac{\beta c}{2} \to 0$, Eq. (20) becomes

$$\dot{x} = x(1-x)\left[-\frac{\beta}{2}c[1-w(x)] + w(x)\right], \tag{22}$$

which has a stable interior equilibrium $x^* = 1 - (1+\frac{\beta c}{2})\ln(1+\frac{\beta c}{2})/(\frac{\beta c}{2}R_0)$. For small c, the first-order approximation of this expression is $1 - \frac{1+\frac{\beta c}{4}}{R_0}$. Comparing this approximation to the Nash equilibrium($x^* = 1 + \ln(1-c)/(cR_0) \approx 1 - \frac{1+c/2}{R_0}$), we note that the effect of large β can be described as rescaling small values of c by a factor of $\frac{\beta}{2}$.

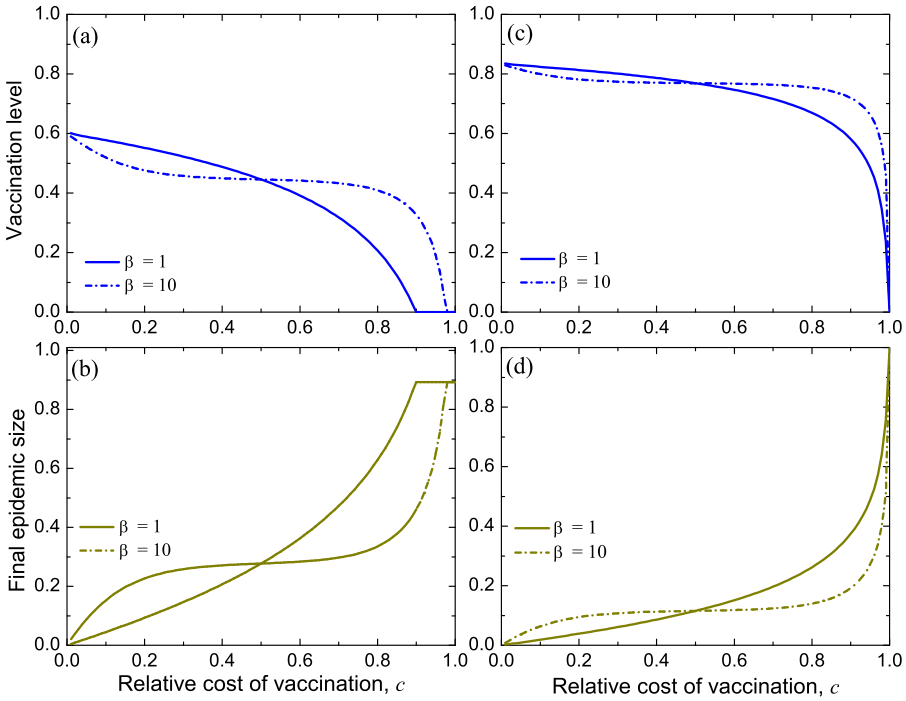

Figure S6: Imitation dynamics in a large, well-mixed population (diffusion approximation). Upper panels (a), (c) show the equilibrium vaccination level, as a function of relative cost of vaccination c with different intensities of selection β. Lower panels (b), (d) show the final epidemic size, as a function of relative cost of vaccination c with different intensities of selection β. Parameters: (a)(b) $R_0 = 2.5$, (c)(d) $R_0 = 6$.

B2. $c \to 1$ $(c > 1 - 1/\beta)$, $-\frac{\beta(1-c)}{2} \to 0$, Eq. (20) becomes

$$\dot{x} = x(1-x)\left\{-[1 - w(x)] + \frac{\beta}{2}(1-c)w(x)\right\}. \tag{23}$$

The third factor in Eq. (23) equals zero for vaccination level $\tilde{x} := 1 - \frac{(2+\beta(1-c))\ln\left(\frac{2+\beta(1-c)}{\beta(1-c)}\right)}{2R_0}$. If this value is positive, then the stable interior equilibrium is $x^* = \tilde{x}$; otherwise, $x^* = 0$.

B3. For intermediate c $(1/\beta < c < 1 - 1/\beta)$, the vaccination level Eq. (20) depends little on β and can be approximated as

$$\dot{x} = x(1-x)[2w(x) - 1], \tag{24}$$

which has a stable interior equilibrium $x^* = 1 - \frac{2\ln 2}{R_0}$. Therefore the vaccination level has a plateau at $1 - \frac{2\ln 2}{R_0}$ for large β and intermediate c values.

Notice that at $c = 0.5$, $x^* = 1 - \frac{2\ln 2}{R_0}$ is an equilibrium for any β value (figure S6).

Figure S6 shows the effects of selection strength β and R_0 on equilibrium vaccination coverage (figure S6a versus S6c) and final epidemic size (figure S6b versus S6d). We can see that for low β the equilibrium vaccination level under imitation dynamics converges to the Nash Equilibrium. Strong selection (large β values) causes the vaccination level to drop below the Nash equilibrium when vaccination cost is low. Furthermore, greater risk of infection (higher R_0) does prompt higher levels of vaccination among imitating individuals, shrinking the gap between the utilitarian optimum and the voluntary outcome (cf. figures S6a and S6c).

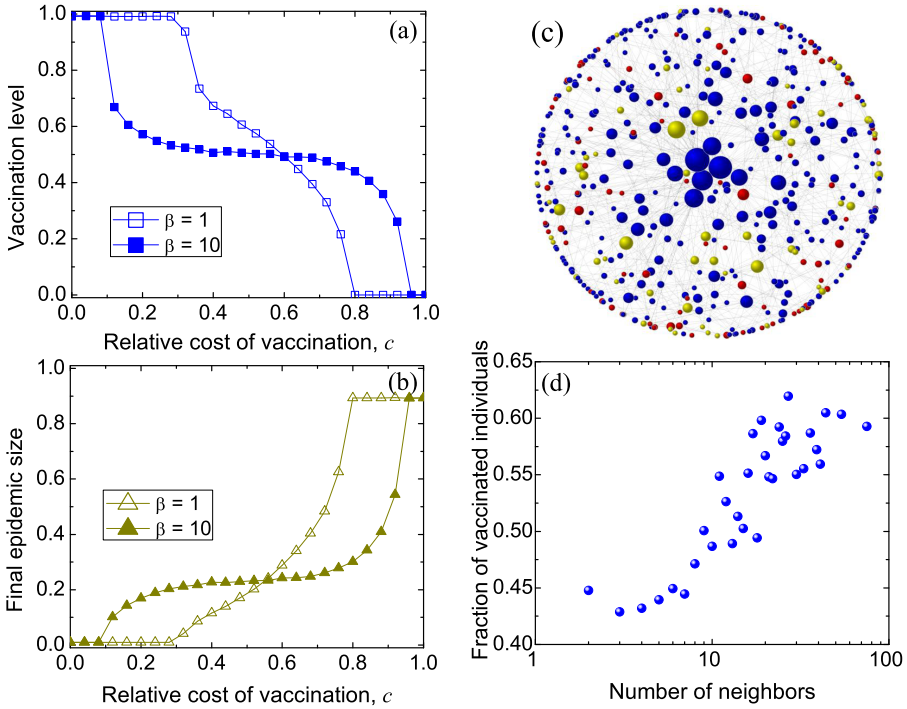

Figure S7: Vaccination dynamics on scale-free networks. Left panels show the fractions of (a) vaccinated and (b) infected individuals as a function of relative cost of vaccination c with the intensity of selection $\beta = 1$ and 10. Right panels: (c) Snapshot of a single simulation on a scale-free network. The size of a node corresponds to its degree. Blue nodes are vaccinated, yellow are infected, and red are successful free-riders. (d) The frequency of vaccination on a scale-free network, as a function of the number of social contacts an individual has (node degree). Parameters: (a)–(d) average degree $\bar{k} = 4$, disease transmission rate $r = 0.55$ day^{-1}person^{-1}, recovery rate $g = 1/3$ day^{-1}, $I_0 = 10$; (a)(b)(d) $N = 1000$, (c) $N = 500$; (c)(d) $c = 0.2$, $\beta = 10$. Results in panels (a), (b), and (d) are averaged over 100 runs. The lines in (a) and (b) are visual guides.

5 Vaccination dynamics on scale-free networks

In addition to random graphs reported in the main text, we consider vaccination dynamics on scale-free networks. The degree distribution of real-life social networks follows a power law, which can be represented using a Barabási-Albert scale-free network model (Barabási & Albert, 1999). Scale-free networks generally possess larger degree heterogeneity than random graphs, leading to more severe persistence of epidemic outbreaks, making herd immunity more difficult to achieve (cf. figures S3 and S4). As a consequence, network heterogeneity further promotes individuals' vaccination on scale-free networks (figure S7). The range of c that promotes 100% vaccination is larger than in the case of random graphs (for $\beta = 1$: $c < 0.3$ for scale-free versus $c < 0.2$ for random; for $\beta = 10$: $c < 0.1$ versus $c < 0.05$).

Despite this difference, the overall pattern of equilibrium vaccination coverage in scale-free networks is similar to that of random networks: "hubs" with many neighbors tend to vaccinate more often than small-degree individuals do (figure S7d). The particular structural characteristics of the Barabási-Albert scale-free network model seem to complicate this pattern slightly, in that the most likely free-riders actually have intermediate degree ($k = 3, 4, 5$ in figure S7d) rather than lowest degree ($k = 2$). Since many degree-two nodes are connected only to large hubs, their vaccination decisions are determined by imitation of these hubs. This peer influence appears to outweigh the fact that they can easily free-ride on the hubs' immunity, increasing the vaccination frequency of degree-two nodes above that of slightly better-connected individuals.

Although degree heterogeneity promotes vaccination, the equilibrium vaccination coverage is still sen-

sitive to the cost of vaccination. Above a critical cost, the vaccination coverage rapidly falls below both the herd immunity threshold (figure S7a) and the final size of the epidemic grows (figure S7b). For influenza, the estimated relative cost of vaccination to infection is less than 0.1, which is approximately the threshold found in the $\beta = 10$ case. Misperceived vaccination risks and individual variation in attitudes towards vaccination may, however, tip the effective value of c above this threshold.

References

Barabási, A. L. & Albert, R. 1999 Emergence of scaling in random networks. *Science* **286**, 509–512.

Erdős, P. & Rényi A. 1959 On random graphs. *Publ. Math. Debrecen* **6**, 290–297.

Galvani, A. P., Reluga, T. C. & Chapman, G. B. 2007 Long-standing influenza vaccination policy is in accord with individual self-interest but not with the utilitarian optimum. *Proc. Natl. Acad. Sci. USA* **104**, 5692–5697.

Gillespie, D. T. 1977 Exact stochastic simulation of coupled chemical reactions. *J. Phys. Chem.* **81**, 2340–2361.

Heffernan, J. M., Smith, R. J. & Wahl, L. M. 2005 Perspectives on the basic reproductive ratio. *J. R. Soc. Interface* **2**, 281–293.

Keeling, M. J. & Eames, K. T. .D. 2005 Networks and epidemic models. *J. R. Soc. Interface* **2**, 295–307.

Hofbauer, J. & Sigmund, K. 1998 *Evolutionary Games and Population Dynamics*. Cambridge, UK: Cambridge University Press.

Newman, M. E. J. 2003 The structure and function of complex networks. *SIAM Review* **45**, 167–256.

Pastor-Satorras, R. & Vespignani, A. Epidemic spreading in scale-free networks. *Phys. Rev. Lett.* **86**, 3200.

Perisic, A. & Bauch, C. T. 2008 Social contact networks and disease eradicability under voluntary vaccination. *PLoS Comp. Biol.* **5**, e1000280.

Traulsen, A., Claussen, J. C. & Hauert, C. 2005 Coevolutionary dynamics: from finite to infinite populations. *Phys. Rev. Lett.* **95**, 238701.

Traulsen, A., Pacheco, J. M. & Nowak, M. A. 2007 Pairwise comparison and selection temperature in evolutionary game dynamics. *J. Theor. Biol.* **246**, 522–529.